J. MACROMOL. SCI.—PURE APPL. CHEM., A38(12), 1231–1243 (2001)

TAILORING TISSUE ENGINEERING SCAFFOLDS USING ELECTROSTATIC PROCESSING TECHNIQUES: A STUDY OF POLY(GLYCOLIC ACID) ELECTROSPINNING

Eugene D. Boland,[1] Gary E. Wnek,[2] David G. Simpson,[3] Kristin J. Pawlowski,[1] and Gary L. Bowlin[1,*]

[1]Department of Biomedical Engineering, P.O. Box 980694,
[2]Department of Chemical Engineering, P.O. Box 843028, and
[3]Department of Anatomy, P.O. Box 980709, Virginia Commonwealth University, Richmond, Virginia 23298

Dedicated to the memory of Professor Sukant K. Tripathy.

ABSTRACT

Poly(glycolic acid) (PGA) has long been a popular polymer in the tissue engineering field. PGA possesses many favorable properties such as biocompatibility, bioabsorbability, and tensile strength. The traditional fiber formation techniques of melt extrusion and cold-drawing are generally limited to fibers of 10-12 μm in diameter. Electrostatic spinning, or electrospinning, is an attractive approach for the production of much smaller diameter fibers which are of interest as tissue engineering scaffolds. We demonstrate the ability to control the fiber diameter of PGA as a function of solution concentration and fiber orientation, as well as show a correlation between the fiber orientation, elastic modulu, and strain to failure of PGA in a uniaxial model.

Key Words: Electrospinning; Tissue Engineering; Scaffold; Poly(Glycolic) Acid

*Corresponding author. Fax: (804) 828-4454; E-mail: glbowlin@saturn.vcu.edu

INTRODUCTION

Poly(glycolic acid), or PGA, is one of a group of biodegradable aliphatic polyesters currently exploited in a variety of medical applications. PGA possesses a moderate degree of crystallinity, a high melting point, and low solubility in organic solvents. Importantly, monofilaments can be degraded *in vivo* in as little as 2 to 4 weeks due to its hydrophilic nature [1, 2].

PGA's inception as a biomaterial came in the 1970's as a degradable suture material. It was found to have better than average tissue compatibility, reproducible mechanical properties such as strength, elongation and knot retention, and predictable bioabsorption [1]. Hydrolytic degradation accounts for the nearly 60% loss of strength during the first two weeks and is characterized by a sharp decrease in local pH and a decrease in crystallinity [3]. This mechanism appears to be applicable to a host of semi-crystalline, bioresorbable polymers [2].

The current commercial process of producing PGA for medical applications is a braiding of multiple melt-spun filaments. These braided, multi-stranded fibers are either used as suture material, such as Dexon™ (American Cyanamid Co., Inc.), or woven into mats such as Medisorb™ (Dupont Co., Inc.) to serve as tissue dressings [1, 2]. These constructs have also been employed as scaffolds in tissue engineering. One limitation of these commercially prepared PGA products is the relatively large fiber sizes (10–12 μm) which are due to the limitations of traditional extrusion [4]. We believe that the proper *in vivo* phenotype cannot be achieved if cells are presented with fibers that possess diameters equal to the cell size or, in many cases, an order of magnitude greater than the cell size. Observational evidence for this conclusion comes from a consideration of the native extracellular matrices of various tissues. Cells appear to have a highly intricate 3-D relationship with their extracellular structures. These structures, which are primarily composed of collagens, exhibit varying fiber diameters which are quite frequently one or more orders of magnitude smaller than the cell itself [5]. This presents a unique problem and challenge for the fabrication of materials to be used as tissue engineering scaffolds.

Electrostatic spinning represents an attractive means to achieve these small fiber diameters. It is of interest to briefly contrast electrospinning with electrostatic spraying, as spraying or spinning can be achieved depending upon the polymer concentration in solution. In electrostatic spraying, or more simply electrospraying, charged droplets are generated at the tip of a metal needle (or pipette with a wire immersed in the liquid) with a several kV dc field, and are subsequently delivered to a grounded target. The droplets are derived by charging a liquid to ca. 5-20 kV (corresponding to electric field strengths of ca. 1,000 V/cm), which leads to charge injection into the liquid from the electrode. The sign of the injected charge depends upon the polarity of the electrode; a negative electrode produces a negatively charged liquid. Electrostatic repulsions within the charged liquid coupled with attraction to the ground electrode of opposite polarity lead to the formation of a so-called Taylor cone at the needle tip. Subsequently, a jet is formed

when electrostatic forces between the charged liquid and the ground exceed the liquid's surface tension. The jet, like any unconfined liquid column, is susceptible to a Rayleigh instability which, in turn, leads to the creation of droplets. If the liquid is relatively volatile, evaporation leads to shrinkage of the droplets and an increase in excess charge density, affording break-up into smaller droplets. The electrospinning phenomenon is mechanistically similar to electrospraying, a key difference being that chain entanglements in more concentrated polymer solutions or melts help to stabilize the initial jet against break-up into droplets. Solvent evaporation (or crystallization from the melt) ultimately stabilizes the jet, the result being a continuous fiber.

While electrospinning has been known for some time [6, 7] and attempts have been made to produce vascular grafts by this technique [8], only recently has interest in electrospinning for polymer biomaterial processing been revived [9-15]. Of particular interest is the ability to generate polymer fibers of sub-micron dimensions, down to about 0.05 microns (50 nm), a size range that is otherwise difficult to access [16]. In electrospinning, polymer solutions or melts are deposited as fibrous mats, with advantage taken of chain entanglements in melts or at sufficiently high polymer concentrations in solution to produce continuous fibers [17]. The basic elements of a laboratory electrospinning system are simply a high voltage supply, collector (ground) electrode/mold, source electrode, and a solution or melt to be sprayed or spun. The sample is confined in any material formed into a nozzle with various tip bore diameters (such as a disposable pipette tip) with a thin source electrode immersed in it. The collector can be a flat plate wire mesh or, in more sophisticated modifications, a rotating metal drum or plate on which the polymer is wound.

With successes seen in the electrospinning of other polymers, it seemed reasonable to believe that this process could be utilized for bioabsorbable polymers as well. Indeed, we recently demonstrated that poly(glycolic acid), poly(l-lactic acid), their copolymers, and collagen are readily electrospun [11-14] and that the products are promising scaffolds for muscle growth and components of engineered vascular grafts. In the present study, we set out to develop protocols that would demonstrate the effects of various control parameters on the electrospinning of PGA. We desired the ability to produce continuous fibers with diameters significantly smaller than those available through commercial extrusion, as well as the ability to tailor the fiber orientation in the electrospun scaffold. We suggest that the combination of these two parameters can drive the mechanical properties of a spun mat that can eventually be used to mimic the natural mechanical and structural properties of a target tissue.

METHODS

The prototype electrospinning process that we employed in this study is described schematically in Figure 1. Jet initiation is achieved by charging a poly-

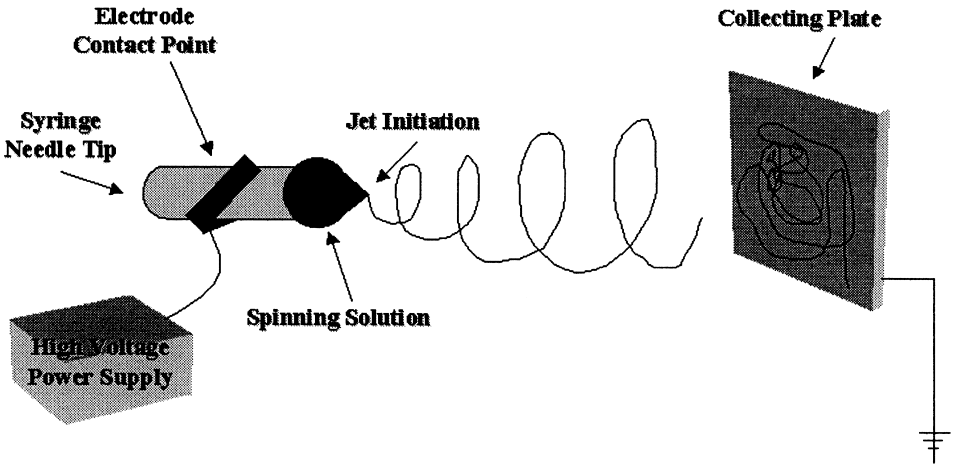

Figure 1. A schematic of the electrospinning system for the production of micro- to nano-scale fibers and subsequent biodegradable polymer tissue engineering scaffolds.

mer solution (or melt) followed by ejection through a small opening or nozzle (a blunt needle in our prototype). Because of its charge, the ejected solution is drawn toward a grounded collecting target (a stainless steel mandrel in our system) as a whipping jet [16]. During the jet's travel, the solvent gradually evaporates leaving a continuous polymer fiber that accumulates on the grounded target. Orientation can be controlled through rotation and translation of the mandrel while collecting the fiber. The charges on the fibers eventually dissipate, as they are neutralized by the surrounding environment [16] or can be neutralized with an ionizer. This process results in the production of a non-woven fibrous mat. These mats can have fiber diameters on the order of nanometers to microns.

For this research, poly(glycolic acid) (100 PGA) obtained from Alkermes, Inc. (Cincinnati, OH) was dissolved in 1,1,1,3,3,3 hexafluoro-2-propanol (HFIPA, Sigma Chemical Co.) at concentrations ranging from 1/7 to 1/20 weight/volume (w/v) of PGA in HFIPA. The solutions were then loaded into a Becton Dickinson 1.0-ml syringe and placed in a KD Scientific syringe pump for metered dispensing at 10 ml/hr. The positive output lead of a high voltage supply (Spellman CZE1000R; Spellman High Voltage Electronics Corp.), set to 22 kV, was attached to a blunt 18 gauge needle on the syringe. A grounded target (1" × 4" × 1/8" 303 Stainless Steel) was placed 11 inches from the needle tip and revolved at 100 RPM for random fibrous mats and 1000 RPM for aligned fibrous mats.

An experimental protocol to test the effect of solution concentration and orientation was desired. All other electrospinning parameters were held constant, including applied voltage, distance between the anode (needle tip) and cathode (grounded mandrel), solution feed rate, HFIPA and PGA manufacturing lots, mandrel material, syringe and needle configuration, translation speed, and rotation speed (within each orientation group). Solution concentrations of 1/7, 1/8,

1/9, 1/10, 1/12, and 1/20 w/v PGA to HFIPA were evaluated. This concentration range was selected from preliminary work done in our laboratory that identified 1/7 w/v PGA to HFIPA as an acceptable spinning solution. By reducing the solution concentrations, a low concentration threshold for spinning this solution could be determined, and the hypothesis that fiber diameter can be controlled in part by solution concentration was investigated. Fiber diameters were determined by scanning electron microscopy (SEM) using a JEOL JSM-820 JE electron microscope. The images were digitized and analyzed by UTHSCSA's ImageTool 2.0 to determine the average fiber diameters (average and standard deviation calculated from 60 measurements per micrograph) in the various mats. All measurements were calibrated using the scale on the micrograph as a reference to avoid errors in calculating the magnification of the scanned photos.

The second hypothesis addressed in this experiment was that the material properties of a mat can be altered by changing the fiber orientation and the spinning solution concentration. As previously mentioned, it is believed that the orientation of the mat can be controlled through rotation and translation of the mandrel and that the diameters of the fibers can be varied by changing the solution concentrations. For this experiment, translation speed was held constant (at 25.4 mm/sec) and the rotation speed was 100 rpm for random mats of all concentrations tested and 1000 rpm for aligned mats of all the concentrations tested. The degree of alignment was visually assessed from SEM micrographs. Future work will involve the implementation of methods to quantify the orientation.

Uniaxial material testing was performed on a MTS Bionix 200 mechanical testing system incorporating a 100N load cell with an extension rate of 1.0 mm/minute to failure (MTS Systems Corp.; Eden Prairie, MN). Due to the viscoelastic nature of PGA, a slow loading rate was chosen to mimic static loading conditions. Five (n = 5) test specimens were tested in each of the following orientations at each solution concentration: Longitudinal – along the principal fiber direction in the aligned mat, Orthogonal – perpendicular to the principal fiber orientation in the aligned mat, and Random – taken from the random mat. The specimens were cut out of the mats using a "dog-bone" shaped template to assure uniformity and to isolate the failure point away from the grips. The specimens had a width of 2.75 mm, a gauge length of 11.25 mm and thicknesses that ranged from 0.6 to 1.25 mm. The material properties chosen for comparison were the elastic modulus (tangential method automatically selected by the MTS TestWorks 4.0 software) and the strain to failure (also calculated automatically by the software).

RESULTS AND DISCUSSION

A strong linear relationship between fiber diameter and concentration in electrospun PGA was observed (Chart 1). Remarkably, the fiber diameters ranged a full order of magnitude from 110 nanometers to 1.19 microns with relatively small error over the concentrations evaluated. Even the largest diameters produced

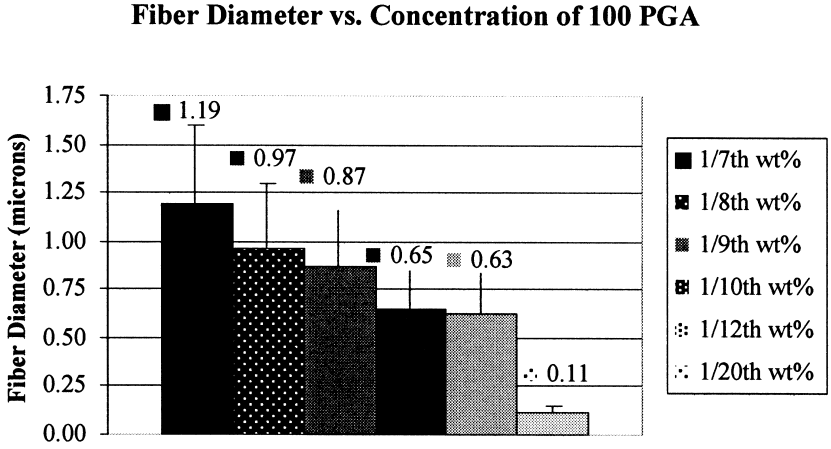

Chart 1. The PGA fiber diameters as a function of solution concentration produced by electrospinning.

by electrospinning are more than 10 times smaller than those that can be extruded to manufacture braided thread and woven mats [4].

The electrospinning results show peak fiber diameters of 1.19 ± 0.41 microns for the 1/7 w/v concentration of PGA in HFIPA. With a drop in concentration to 1/10 w/v (4.3% drop in concentration), the mean fiber diameters drop to 0.65 ± 0.21 microns (45.4% drop in mean diameter). This trend continues between the 1/10 w/v concentration and the 1/20 w/v concentration (5% drop in concentration), since the mean fiber diameter drops to 0.11 ± 0.04 microns (83% drop in mean diameter). A curve fit of these data (Chart 2) could be used predict the con-

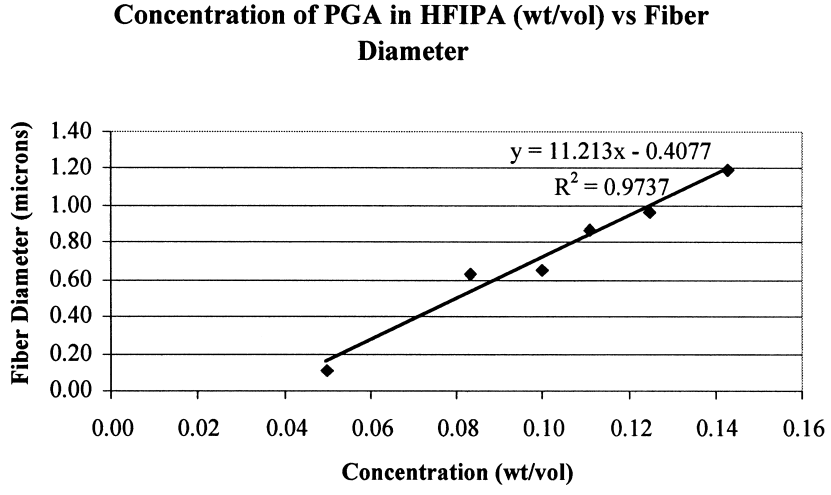

Chart 2. A linear regression of the concentration of PGA in HFIPA vs. the fiber diameter. The R^2 value of 0.9737 supports the correlation hypothesis.

centration needed to produce a desired fiber diameter within the concentration range that is capable of being spun. This equation (Diameter (microns) = 11.213 ∗ concentration (wt/vol) – 0.4077) is valid only at the experimental conditions listed in this protocol and would need to be regenerated for any additional polymer/polymer blend or protocol of interest.

The results clearly support the first hypothesis of a significant ($R^2 = 0.9737$) dependence of fiber diameter on concentration. The low concentration threshold was also determined to be at or near 1/20 w/v. As previously stated, when the solution concentration drops, electrostatic spinning reverts to the historically described electrostatic spraying discussed earlier. A threshold is defined as the observance of three distinct product morphologies: the presence of fibers, a phenomenon termed "beads on a string", and the presence of droplets resulting from electrospraying [12, 13].

Figure 2 shows a representative sample of these three morphologies. The true threshold would be the concentration at which a further reduction would first cause "beads on a string" to form. This transitional region, as illustrated in Figure 2, has a gradual increase in beads and droplets until no more fibers form. This concentration would define the upper threshold of electrospraying, or the lower threshold of electrospinning.

Figure 3 is a higher magnification view of the same mat spun from a 1/20 w/v solution. From this micrograph, we can see that there is a high degree of uniformity in the fibers aside from the bead formation. This leads to the conclusion that bead formation may be a localized effect, possibly caused by variation in field strength or localized solution concentration in the needle tip, and may not grossly

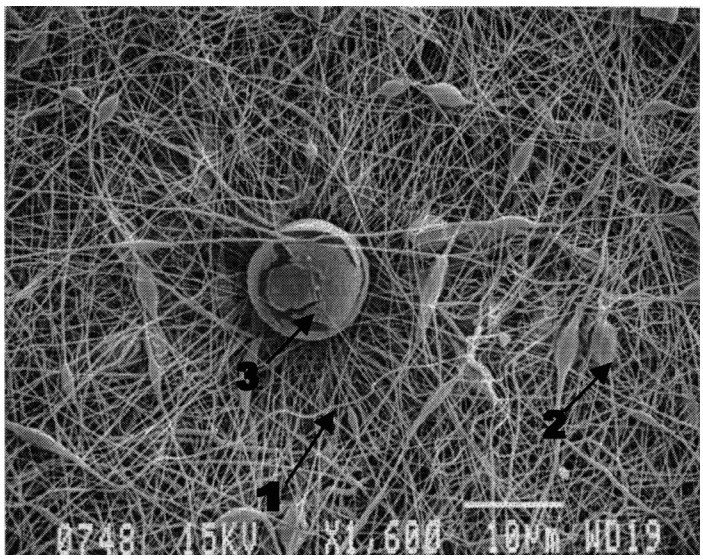

Figure 2. A SEM of electrospun PGA illustrating (1) Fibers, (2) "beads on a string", and a (3) droplet (ruptured during SEM scan) (1,600X magnification).

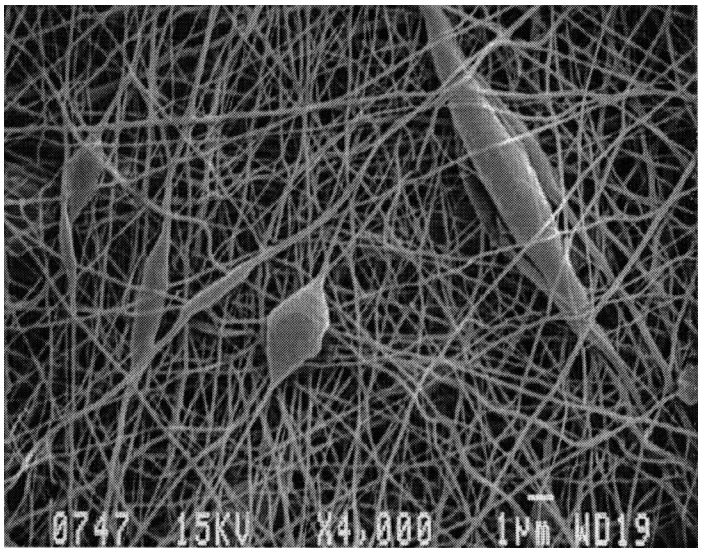

Figure 3. A SEM micrograph (4,000X magnification) of 1/20 w/v concentration of PGA in HFIPA illustrating the fiber size uniformity (110 ± 35 nm).

affect the properties of the scaffold if the density of beads is low. Future mechanical testing at and just below the spinning threshold will test this hypothesis.

After biocompatibility and tissue incorporation are addressed, traditional engineering principals such as stress and strain may ultimately govern the success of a tissue engineering scaffold [18]. The mechanical properties of interest in this study were the modulus of elasticity and strain at failure. We believe that these are two of the key characteristic properties that must be addressed in the design of a structural tissue engineering scaffold. These characteristics, together with maximum stress, are commonly reported for soft tissues in various literature and will form a basis of comparison for future work.

Figures 4a and 4b exemplify the ability to align the fibers in a spun mat. The only variable changed between the two mats is the rotational velocity of the mandrel picking up the fiber that is whipping around within the developed static electric field.

As evidenced by the micrographs in Figure 4, a visual distinction can be made between the aligned and random mats. Also evident is the incomplete alignment seen in Figure 4a. As previously discussed, a method for quantifying the orientation will be needed to compare scaffold orientation with the native tissue orientation. Future studies will address this issue.

Elastic moduli calculations were made and averaged from 15 groups (5 specimens from each test category). The results of these calculations are shown in Chart 3. A statistical analysis comparing the moduli at the different orientations and concentrations was performed using the Student's T-test. The 1/7 w/v concentration showed a significant difference between the longitudinal and orthogonal

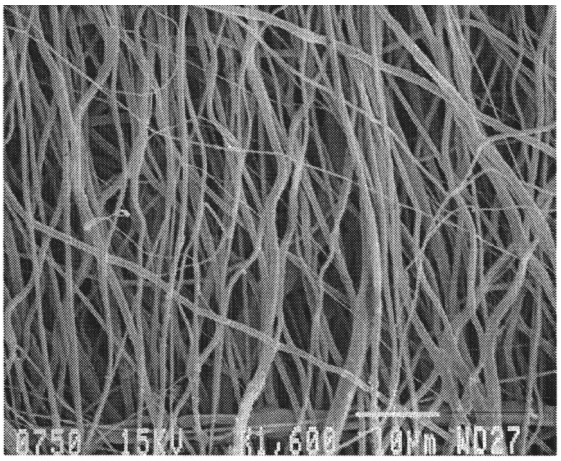

(a)

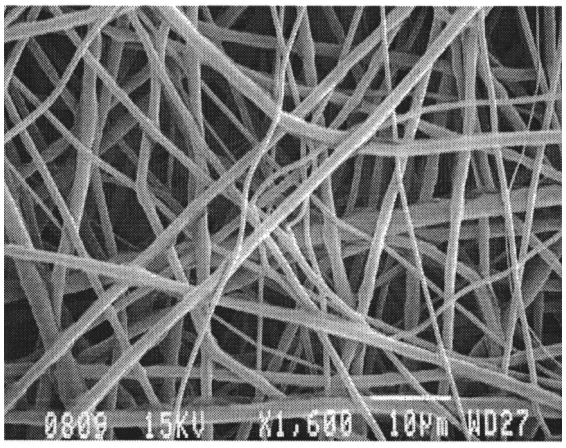

(b)

Figure 4. (a) Electrospun 1/7 w/v PGA in HFIPA illustrating aligned fibers (mandrel rotation of 1000 rpm), (b) Electrospun 1/7 w/v PGA in HFIPA showing the random fiber orientation (mandrel rotation of 100 rpm). Both micrographs are at 1,600X magnification.

directions ($P < 0.001$) and between the longitudinal and random directions ($P < 0.001$). The 1/8 w/v concentration showed a significant difference between the longitudinal and orthogonal directions ($P < 0.001$) and between the orthogonal and random directions ($P < 0.001$). The 1/9 w/v concentration showed a significant difference between the longitudinal and orthogonal directions ($P < 0.001$) and between the longitudinal and random directions ($P < 0.001$). The 1/10 w/v concentration showed a significant difference between the longitudinal and orthogonal directions ($P < 0.001$) and between the longitudinal and random directions ($P <$

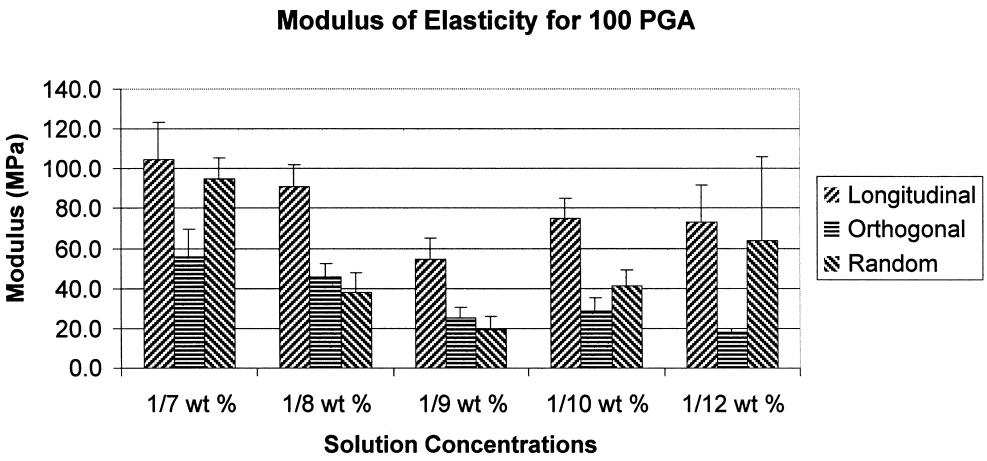

Chart 3. Tangential modulus of elasticity for various concentrations of PGA tested along the longitudinal and orthogonal axes and in a random mat.

0.005). The 1/12 w/v concentration showed a significant difference only between the longitudinal and orthogonal directions ($P < 0.005$). The *a priori* level of significance for all tests was set equal to $P < 0.01$. Generalizing for elastic moduli testing, the longitudinal direction always possessed a greater stiffness than the orthogonal direction, and the random scaffolds typically exhibited moduli similar to either the longitudinal or the orthogonal directions.

A similar T-test was performed to compare the modulus of a particular orientation to the solution concentrations. Significant differences in the longitudinal direction were found only at 1/7 w/v ($P < 0.005$). Similarly, only the 1/9 w/v yielded a significant difference in the orthogonal direction ($P < 0.005$). In the random orientation, both the 1/7 w/v concentration ($P < 0.005$) and the 1/9 w/v concentration ($P < 0.001$) were significantly different. These statistical tests support the hypothesis that strength is a function of orientation.

The highest modulus of 104.9 MPa was seen along the longitudinal axis of the 1/7 w/v concentration. This would follow reason since the fiber diameters are the greatest and the alignment would present the maximum resistance. The lowest moduli were observed along the orthogonal axis for most of the concentrations, again, as expected.

Additionally, the peak strains were calculated from the same sample groups with the results presented in Chart 4. All five solution concentrations produced equivalent results with the strain to failure being highest for the orthogonal specimens and lowest for the longitudinal specimens. A Student's T-test was performed to compare the strain to failure of the mats at the three orientations to the solution concentrations. The only significant differences were seen in the 1/7 w/v concentration ($P < 0.001$) and the 1/8 w/v concentration ($P < 0.005$) in the random orientation. This also correlates to the suspected orientation in the mats since strain values are higher when the specimens are not loaded along the principal axis of the

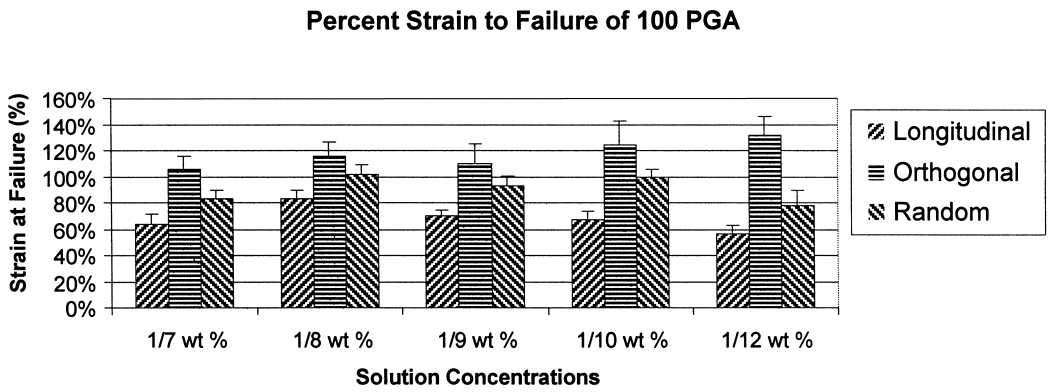

Chart 4. Maximum strain measurements for various concentrations of PGA.

fibers but are similar across the solution concentrations. Future studies with larger sample sizes are needed to verify the difference measured in the 1/7 and 1/8 w/v concentrations.

The ensemble average of engineering stress versus strain is included in Chart 5 for the 1/7 w/v concentration along the longitudinal and orthogonal axes and with random orientation. This chart is included to illustrate the general mechanical response as a function of fiber orientation. It is evident that the stress handling ability of the mat is related to the degree of orientation. Energy or toughness (area under the load - elongation curve) is another measurement that can be used to compare bulk mechanical properties of the scaffolds. The toughness values for the 1/7 w/v concentrations are 10.2 N*mm, 11.2 N*mm, and 11.8 N*mm, respec-

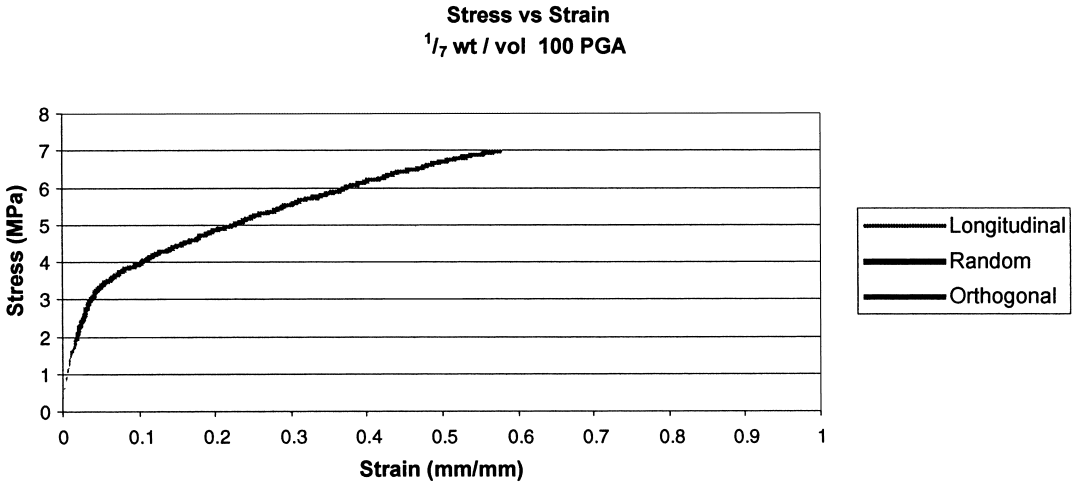

Chart 5. Ensemble Averaged Stress vs. Strain Plot for all Three Orientations of 1/7 Wt/Vol Concentration of PGA.

tively, for the longitudinal, orthogonal, and random orientations. A Student's T-Test was performed, and there was no significant difference between these values (significance $P < 0.1$). This is as expected since the energy a material can absorb before failure is a fundamental material property dependent principally on composition and processing. Similar results were achieved in the comparison of energy versus orientation for the remaining test concentrations of PGA in HFIPA. Paired T-Tests were computed comparing the energy of each orientation and concentration, and, again no significant differences were found (significance $P < 0.1$).

Through the course of these experiments, the ability to electrostatically process PGA was demonstrated at various concentrations. These concentrations were directly related to the fiber diameters produced via the process. The fiber scale achieved was one to two orders of magnitude smaller than commercially available fibers. Future cell culture experiments will be needed to determine if creating smaller diameter fibers in a scaffold is just novelty or improves phenotypic expression or construct viability. One may argue that that pore sizes in these scaffolds are too small to promote tissue ingrowth or vascularization. However, there may be other factors at work with cell migration, as we have demonstrated (unpublished data) that cells (smooth muscle cells) can migrate into a scaffold with pore sizes less than the previously reported 10 micron threshold.

When reviewing the alignment of the mats depicted, it is apparent that the alignment is not 100%. Refinement of the aligning process will be undertaken through the implementation of additional control on the mandrel rotation and location (next generation electrospinning apparatus). This will be accomplished by an advanced processing system, and will provide the critical next step in our ability to tailor scaffolds that truly mimic the target tissue.

After alignment is achieved, the tissue mechanics will need to be satisfied. Clear trends were shown in the strain to failure and elastic modulus of the various constructs. As mentioned previously, the orthogonal and random orientations of 1/8 and 1/9 w/v concentrations did not follow the pattern of the other concentrations. One possible reason for the deviation could be the quality of alignment of the scaffold. While these appear aligned by visual examination, there may be underlying fibers which are not aligned. Another, and more probable, reason is that the solvent used for the solutions (HFIPA) did not fully evaporate and we saw the effect of solvent bonding or welding which would make the orthogonal and random mats structurally similar.

CONCLUSION

Poly(glycolic acid) is readily electrospun to afford fibers ranging from about 0.15 to 1.5 μm in diameter, the latter being related to the concentration of the spinning solution. Oriented electrospun mats were achieved using a rotating collection plate, and mechanical testing revealed anisotropic properties of the oriented mats. We believe that the fine fiber diameters make electrospun PGA an attractive can-

didate as a tissue engineering scaffold, and experiments are underway to evaluate this prospect.

ACKNOWLEDGMENTS

The authors would like to thank the Whitaker Foundation (RG-98-0465) for the support of this research, as well as Alkermes, Inc., for the donation of the PGA used in this study. We would also like to thank Ms. Judy Williamson for her assistance obtaining the SEM micrographs.

REFERENCES

1. Wong, W.H.; Mooney, D.J. *Synthetic Biodegradable Polymer Scaffolds*. Atala, A.; Mooney, D.; Vacanti, J.P.; Langer, R., Eds. Birhauser: Boston, MA.; 1997, 50.
2. Barrows, T.H. *High Performance Biomaterials: A Comprehensive Guide to Medical and Pharmaceutical Applications*, M. Szycher, Ed., Technomic: Lancaster, PA; 1991, 243-57.
3. Chu, C.C.; Browning, A. J. Biomed. Matr. Res. **1998**, *22*, 699.
4. Mooney, D.J.; Langer, R.S. *The Biomaterials Handbook*, CRC Press: Boca Raton, FL; 1995, pp. 1609-1618.
5. Olsen, B.R. In, *Principles of Tissue Engineering*, Lanza, R.; Langer, R.; Chick, W., Eds. Academic Press: San Diego, CA; 1997, 47.
6. Formhals. A. U.S. 1,975,504, 1934.
7. Baumgarten, P.K. J. Coll. Interface Sci. **1971**, *36*, 71.
8. Martin, G.E.; Cockshott, I. D. U. S. 4,043,331, 1977.
9. Buchko, C.J.; Chen, L.C.; Shen, Y.; Martin, D.C. Polymer **1999**, *40*, 7397.
10. Huang, L.; McMillan, R.A.; Apkarian, R.P.; Pourdeyhimi, B.; Conticello, V.P.; Chaikoff, E.L. Macromolecules **2000**, *33*, 2989.
11. Stitzel, J.D.; Bowlin, G.L.; Mansfield, K.; Wnek, G.E.; Simpson, D.G. *Proc. 32nd Ann. SAMPE Meeting,* Boston, 2000, pp. 205-211.
12. Stitzel, J.D.; Pawlowski, K.; Wnek, G.E.; Simpson, D.G.; Bowlin, G.L. J. Biomater. Appl., in press.
13. Matthews, J.A.; Wnek, G.E.; Simpson, D.G.; Bowlin, G.L. Biomacromolecules, in press.
14. Bowlin, G.L.; Pawlowski, K.J.; Stitzel, J.D.; Boland, E.D.; Simpson, D.G.; Fenn J.B.; Wnek, G.E. In, *Tissue Engineering and Biodegradable Equivalents: Scientific and Clinical Applications*, Wise, D.L.; Lewandrowski, K.; Trantolo, D.J.; Gresser, J.D.; Yaszemski, M. J.; Altobelli, D.E., Eds., Marcel Dekker: New York (in press).
15. Bognitzki, M.; Czado, W.; Frese, T.; Schaper, A.; Hellwig, M.; Steinhart, M.; Greiner, A.; Wendorff, J.H. Adv. Mater. **2001**, *13*, 70.
16. Reneker, D.H.; Chun, I. *Nanotechnology* **1996**, *7*, 216-23.
17. Reneker, D.H.; Yarin, A.L.; Fong, H.; Koombhongse, S. J. Appl. Phys. **2000**, *87*, 4531-47.
18. Bell, E. J. Cell. Biochem. **1991**, *45*, 239.